Polar Biol (2015) 38:1727–1740
DOI 10.1007/s00300-015-1738-4

ORIGINAL PAPER

A transcriptomic analysis of the response of the arctic pteropod *Limacina helicina* to carbon dioxide-driven seawater acidification

Hye Yeon Koh[1,3] · Jun Hyuck Lee[1,2] · Se Jong Han[1,2] · Hyun Park[1,2] · Seung Chul Shin[1] · Sung Gu Lee[1,2]

Received: 13 January 2015 / Revised: 9 June 2015 / Accepted: 9 June 2015 / Published online: 17 June 2015

Abstract Ocean acidification from the uptake of anthropogenic carbon dioxide (CO_2) is regarded as a critical threat particularly to marine calcifying organisms. The arctic pteropod *Limacina helicina* may be one of the first polar organisms that are expected to display early sensitivity to ocean acidification, but a molecular approach as a foundation for understanding the effect of ocean acidification on this pteropod has rarely been reported. In this study, we examined the sublethal effects of CO_2-driven seawater acidification at the transcriptome level in *L. helicina*. cDNAs, treated under control (pH 8.2), high-CO_2 (pH 7.5), and extreme-CO_2 (pH 6.5) conditions, generated a total of 31,999,474 reads, comprising a total of 2,271,962,654 bp, using the Illumina platform. De novo assembly yielded 53,121 transcripts comprising 31.79 Mbp. Among the upregulated genes, 346 (0.7 %) and 655 (1.2 %) genes responded to extreme-level CO_2 (pH 6.5) and high-level CO_2 (pH 7.5), respectively. Also, 76 (0.1 %) transcripts were commonly upregulated in both conditions. Among the downregulated genes, 690 (1.3 %) and 739 (1.4 %) genes were in response to extreme-level CO_2 and high-level CO_2, respectively. Also, 270 downregulated genes (0.5 %) were affected in both acidic stress conditions. Moreover, 504 transcripts (1 %) of biomineralization-related genes were identified; 16 of these genes showed differential expression in response to acidified seawater. The dataset provides the first comprehensive overview of changes in transcript levels in the arctic pteropod *L. helicina* in response to increased CO_2, emphasizing the potential impact of future environmental change and ocean acidification on Arctic species with external calcified structures.

Keywords *Limacina helicina* · Pteropod · Transcriptome · Arctic · Ocean acidification · Carbon dioxide · Biomineralization

Introduction

Nearly one-third of the total carbon dioxide (CO_2) released into the atmosphere by human activities has been introduced to the oceans over the past 200 years (Sabine et al. 2004). This CO_2 absorption leads to ocean acidification (lowering seawater pH) and has been regarded as a critical threat, particularly for marine calcifying organisms (Orr et al. 2005a; Doney et al. 2009). Antarctic planktonic foraminifera shell weights have diminished by over 30 % since the late 1800s (Moy et al. 2009), and other marine calcifiers, such as phytoplankton, coralline algae, corals, mollusks, and crustaceans, have shown reduced calcification (Gattuso et al. 1998; Riebesell et al. 2000; Langdon and Atkinson 2005; Gazeau et al. 2007). Calcifiers play an important role in carbon cycling in marine ecosystems by

Electronic supplementary material The online version of this article (doi:10.1007/s00300-015-1738-4) contains supplementary material, which is available to authorized users.

✉ Hyun Park
hpark@kopri.re.kr

✉ Seung Chul Shin
ssc@kopri.re.kr

✉ Sung Gu Lee
holynine@kopri.re.kr

[1] Division of Polar Life Sciences, Korea Polar Research Institute, Incheon, South Korea

[2] Department of Polar Sciences, University of Science and Technology, Incheon, South Korea

[3] Department of Applied Marine Biotechnology and Engineering, Gangneung-Wonju National University, Gangneung, South Korea

calcifying their skeletons, and the saturation state of calcium carbonate ($CaCO_3$) affects their calcification rates (Leng et al. 2013). Aragonite, the more soluble metastable form of $CaCO_3$ (than calcite) in seawater, is used preferentially by most calcifiers; consequently, undersaturation of $CaCO_3$ driven by CO_2 uptake in the marine environment may cause incomplete skeletons (Orr et al. 2005b). Moreover, in addition to affecting calcification, marine acidification can alter growth (Harris et al. 1999; Michaelidis et al. 2005; Shirayama and Thornton 2005; Berge et al. 2006; Hauton et al. 2009), metabolism (Reipschläger and Pörtner 1996; Pörtner et al. 1998; Rosa and Seibel 2008), reproduction and development (Kurihara and Shirayama 2004; Kurihara et al. 2007; Dupont et al. 2008), survival (Watanabe et al. 2006; Dupont et al. 2008), and photosynthesis (Fu et al. 2007) in marine organisms.

Limacina helicina, a thecosomatous pteropod, is a prominent member of the marine zooplankton community, present in high densities in both the Arctic (*L. helicina*) and Antarctic (*L. helicina antarctica*) Oceans (Lalli and Gilmer 1989; Hunt et al. 2008). They are often referred to as 'sea butterflies' because they have evolved their gastropod foot into a pair of wing-like parapodia that allow them a pelagic distribution (Lalli and Gilmer 1989). They are omnivorous and filter-feed by excreting large mucous webs to catch their prey, including phytoplankton and small zooplankton, or even their juveniles (Gilmer and Harbison 1986, 1991; Gannefors et al. 2005). *Limacina helicina* is also a major dietary component for other organisms in marine food webs, such as larger carnivorous zooplankton, for example, ctenophores (Larson and Harbison 1989), *Clione limacina* (Conover and Lalli 1972), and higher predators, including fish, sea birds, and whales (Hunt et al. 2008; Karnovsky et al. 2008).

Limacina helicina produce a sinistrally coiled $CaCO_3$ shell and may be significant contributors to the carbonate export and organic carbon flux (Berner and Honjo 1981; Collier et al. 2000; Hunt et al. 2008). This pteropod species is the only shelled example in Arctic seawater, and the potential impact of Arctic Ocean acidification on high-latitude marine ecosystems is of great concern. *Limacina helicina* has been suggested as one of the first polar organisms to be affected by ocean acidification and thus an indicator species of the impact of such acidification (Fabry et al. 2008). A previous study demonstrated that shell synthesis in the Arctic pteropod, *L. helicina,* is very sensitive to acidic seawater, showing a 28 % decrease in calcification (Comeau et al. 2009). The same authors demonstrated that the calcification rate is affected by pCO_2 levels and temperature by measuring calcium carbonate precipitation based on ^{45}Ca uptake (Comeau et al. 2010). It is anticipated that shells of pteropods could be severely damaged by 2050 along the northern and central onshore California Current Ecosystem (CCE) (Bednarsek et al. 2014). Furthermore, ocean acidification and associated environmental changes, such as global warming, can alter the energetic status of zooplanktons and may sustain metabolic suppression (Seibel et al. 2012). Recent studies carried out a microarray-based transcriptomic analysis of an intertidal larval sea urchin in the Northeast Pacific Ocean (*Strongylocentrotus purpuratus*) and revealed that gene expression in biomineralization, cellular stress response, metabolism, apoptosis, calcium homeostasis, ion transport, cell signaling, and transcription processes were differentially regulated in response to ocean acidification (Todgham and Hofmann 2009; Evans et al. 2013). It was also shown that ocean acidification changes the expression of genes involved in central carbon metabolism, light physiology, signal transduction, and ion transport in the most abundant coccolithophore *Emiliania huxleyi* (Rokitta et al. 2012). It is important to point out that ocean acidification is just one of many challenges and that changes in the mass of pteropod shells in at least one field study do not strictly follow predictions based on aragonite saturation state of seawater (Roberts et al. 2014). Thus, it is clear that understanding the susceptibility of pteropods to global climate change requires the ability to track transcriptomic responses to a complex set of environmental variables, of which acidification is only one.

In this study, we performed gene expression profiling in *L. helicina* to (1) provide a transcriptomic tool as a foundation for research on the susceptibility of pteropods to global climate change and (2) to gain insight into the molecular mechanisms that might be influenced by future ocean acidification in pteropods. For the latter of these, we examined sublethal effects of CO_2-driven seawater acidification at the transcriptomic level in *L. helicina* and evaluated the molecular responses involved in the capacity of the pteropod to respond to future climate change and, more specifically, the potential impact of ocean acidification driven by CO_2.

Materials and methods

Sampling and experimental setup

Limacina helicina was collected at the harbor in Ny-Ålesund in June 2011. Jars mounted on sticks were used to collect pteropods swimming near the water surface, and only undamaged individuals were used for the experiments. The thin and fragile shell of *L. helicina* is easily damaged

or broken, and the thin parapodia are often torn or ripped off when captured using nets (Hamner et al. 1975; Gilmer 1990). The captured *L. helicina* were immediately transported to the Dasan station in Ny-Alesund and sorted according to size. *Limacina helicina* of the same size range (3–4 mm) were then transferred into 4-L beakers, which contained prechilled seawater in a cold chamber set to 0 °C, and kept for 3 days for acclimation to the laboratory environment and gut clearance. The seawater used was filtered through GF/B filters. The seawater was collected from the same site at which the animals were caught. Experimental pH was achieved by CO_2 bubbling into the seawater using pure CO_2. The pH was measured using a pH meter with a glass electrode (Thermo Orion 3 star pH Benchtop) after calibrating with pH buffer solution (certified traceable to NIST standard Reference Material, Thermo Orion) at 0 °C. The acidified seawater was filled up, and the pteropods were placed in 4-L jars (5 individuals/4-L), closed with an air-tight lid, and then stored in a cold chamber set to 0 °C. The acidified seawater was exchanged every 12 h. The pHs were set to 8.23 (control natural seawater), 7.5 (high CO_2), and 6.5 (extreme CO_2). The pHs were measured before every water exchange to monitor any pH fluctuations. The variation of seawater pH levels over time (measured every 12 h) was within 0.05 pH units (data not shown). Five independent replicates were set up in each of the five 4-L chambers for each of the three different pH treatments. After 96 h, the experiment was stopped. The animals were not fed during the experiments due to the short duration (96 h). After termination of the treatments, the shells of pteropods from both acidified seawater were damaged as shown in previous study (Lischka et al. 2011). The animals from the acidified seawater showed barely active movements, but none exhibited mortality. This study, including sample collection and experimental research conducted on animals, was performed according to the law on activities and environmental protection to the Arctic approved by the Minister of Foreign Affairs and Trade of the Republic of Korea.

RNA extraction and transcriptome sequencing

Total cellular RNA was isolated from at least four combined animals of each treatment using the Easy Blue kit (Intron Biotechnology, Korea) according to the manufacturer's instructions, followed by resuspending dried total RNA pellets in 0.1-mL nuclease-free water. To precipitate RNA, 0.1 volume of 3 M sodium acetate, pH 5.0, and 2.5 volume of 100 % ethanol was added to the eluted RNA, mixed by vortexing, and incubated for 1 h at −80 °C. The tubes were then centrifuged (12,000*g*, 20 min, 4 °C). Pellets were rinsed twice with 80 % ethanol and redissolved in 30 µL of nuclease-free water. RNA was quantified spectrophotometrically using a ND-1000 UV/visible spectrophotometer (NanoDrop Technologies, Wilmington, DE, USA) and electrophoresed on a 1.5 % w/v agarose gel to verify RNA integrity. The purified RNA was stored at −80 °C. Total RNA (~10 µg) from each of the three samples was used for sequencing on an Illumina Genome Analyzer II (Illumina, CA, USA) at DNA Link Inc. (Seoul, Korea) according to the manufacturer's protocol.

De novo assembly and functional annotation

The reads were cleaned up with the FastX toolkit software, trimming low-quality ends and adapter sequences, and discarding reads shorter than 50 bp. De novo assembly of the clean reads was conducted using the Trinity software version Trinityrnaseq_r2013-11-10 (Grabherr et al. 2011) in single-end mode with options '-min_-kmer_cov = 2.' The filtered transcripts were annotated with Blast2GO (ver. 2.4.4, http://www.blast2go.com/), a tool developed specifically for the annotation of novel sequence sets (Conesa et al. 2005). Sequence similarity was evaluated with BLASTx [69] against the NCBI nonredundant (nr) protein database using an e-value cutoff of 1×10^{-5} and HSP length cutoff of 33. The presence of conserved domains was researched and annotated using InterProScan (Quevillon et al. 2005) on the six possible translation frames of each transcript. Transcripts were annotated functionally according to the Gene Ontology (GO, http://www.geneontology.org/) nomenclature. GO mapping and annotation were performed with an annotation cutoff of 10^{-5}.

Differentially expressed gene (DEG) analysis of transcripts

The gene expression level from RNA-Seq was normalized to the number of reads per kilobase of exon region per million mapped reads (RPKM). The cutoff value for determining gene transcriptional activity was determined based on the 95 % confidence interval for all RPKM values for each gene. Using scripts included in the Trinity package suite (Grabherr et al. 2011), cleaned reads were aligned to the Trinity-assembled transcripts using Bowtie (Langmead et al. 2009). Transcript abundance was then estimated using the RSEM software package (Li and Dewey 2011). The EBSeq nested in RSEM (Leng et al. 2013), which is a Bayesian hierarchical model for the inference on the differential gene expression based on RNA-seq data, was used to identify genes. To adjust library sizes and skewed expression of transcripts, the estimated abundance values were normalized using the Trimmed Mean of M-values (TMM) normalization method (Robinson and Oshlack

2010), included in EBSeq. DEGs between control and CO_2-driven acidic seawater *L. helicina* samples were identified.

GO enrichment analysis

GO enrichment analysis was carried out using the online 'AgriGO' (http://bioinfo.cau.edu.cn/agriGO/analysis.php) (Du et al. 2010), a web-based GO analysis toolkit with a Fisher's exact test with a threshold of 0.05. False discovery rate (FDR) correction was used with a threshold of 0.05 to reduce false-positive predictions of enriched GO terms.

Quantitative real-time PCR (qRT-PCR)

Results from the DEG analysis were validated by measuring mRNA expression in the same RNA samples from the control and CO_2-driven acidic pH groups using qRT-PCR. RNA samples were treated with deoxyribonuclease I (Sigma, Seoul, Korea) to remove any contaminating genomic DNA. Single-stranded cDNA was obtained by reverse transcription using 2-μg total RNA in a final volume of 20 μL with oligo-dT primers and M-MLV transcriptase (Enzymomics, Korea) according to the manufacturer's instructions. The reaction sequence was 70 °C for 5 min, 42 °C for 60 min, and then terminated by heating to 70 °C for 15 min. cDNA was stored at −20 °C until required for qRT-PCR. Gene-specific primers were designed based on the contig sequences (Table 1). Specific primers amplifying ~100–200-bp PCR products were chosen to validate the DEG data. qRT-PCRs were performed using 2-μL cDNA, 5 pmol of each primer, and SYBR Premix Ex Taq DNA polymerase (Takara, Seoul, Korea) in a total volume of 20 μL using the Mx3000P Real-Time PCR System (Stratagene, La Jolla, CA, USA). All qRT-PCRs were run as follows: 95 °C for 5 min, followed by 40 cycles of 95 °C for 5 s, 55 °C for 20 s, 72 °C for 15 s, and one cycle of 95 °C for 15 s, 55 °C for 1 min, and 95 °C for 30 s. At the end of each PCR, PCR products were subjected to a melt curve analysis to confirm the presence of a single amplicon. The threshold cycle (CT) values, representing the PCR cycle at which fluorescence passed the threshold, were generated using the MxPro-Mx3000P software. All data were normalized against the expression of the reference β-actin gene. The relative expression levels were calculated using the comparative 'ΔΔCT' method. The mean expression values were calculated from triplicate measurements of each target gene. Excel (Microsoft, Redmond, USA) was used for the statistical analysis of qRT-PCR results. Student's *t* test was used to determine significant differences, accepting $P < 0.05$ as significant. Results are expressed as mean ± SD.

Results

Data processing and sequence assembly

cDNA from each *L. helicina*, treated under control (pH 8.23), high-CO_2 (pH 7.5), and extreme-CO_2 (pH 6.5) conditions, was subjected to next-generation sequencing using an Illumina Genome Analyzer II. After removing low-quality regions, adaptors, and possible contaminants, 10,415,488 high-quality reads in the control group, 10,331,415 high-quality reads in the pH 7.5 group, and 11,252,571 high-quality reads in the pH 6.5 group were obtained. Ultimately, in total, 31,999,474 reads, comprising a total of 2,271,962,654 bp, were obtained (Table 2). After de novo assembly with trimmed reads using the Trinity software, size-selected reads were assembled into 53,121 transcripts comprising 31.79 Mbp (Table 3). The transcripts ranged in size from 200 to 12,358 bp with an average size of 599 bp and 796 of N50. The size distribution of the reads is indicated in Fig. 1. All high-quality

Table 2 Summary of reads from each *Limacina helicina* sample, obtained using the Illumina GAII

	Total number of reads	Total bp
Control (pH 8.2)	10,415,488	739,499,648
High-CO_2 (pH 7.5)	10,331,415	733,530,465
Extreme-CO_2 (pH 6.5)	11,252,571	798,932,541
Total	31,999,474	2,271,962,654

Table 1 Sequences of the gene-specific primers used in qRT-PCR

Gene	Forward primer (5′ → 3′)	Reverse primer (5′ → 3′)
Plasminogen	GGTGATCTTCGTGCTTGAAATG	CACAGGAGCAAGTCAAACTATCT
α-Amylase	GCGATGAAGGCTTTGTTTCC	ATGGCCTTCCGCAACAT
C-type lectin	GGTCGGTAACCCTCATCTATTC	GGGACCGATGAGAACTGTATG
Rac 1	GTTGGGTACCAAGCTCGATTTA	TACCTCACTGCCTTGATCTCT
Cathepsin D	GGACTTGGTGGAGTCGTATTT	AGCCCTTCAACGTCATCTTC
Collagen alpha-6	ACTGATGGGAGGTCTACTGAA	GTTGCCAACACCAACAGTAATC
β-actin	TCCTCTCACTGTACGCTTCT	GGGAGAGCATAACCCTCATAGA

reads have been deposited in the NCBI and can be accessed in the Short Read Archive (SRA) under accession number SRP032826 (http://www.ncbi.nlm.nih.gov/).

Functional classification of *L. helicina* transcriptome

The BLAST-matched contigs were assigned with GO terms using the Blast2GO platform. Among the transcripts, 18,324 (34.5 %) sequences were annotated with BLASTx, whereas 34,797 (65.5 %) sequences showed no hits by BLASTx searching (Table 4). The *L. helicina* gene data set was analyzed to identify sequences conserved in other species. The top-hit species distribution of BLAST matches to the 'nr' protein database is shown in Fig. 2. The highest number of *L. helicina* sequences showed homology to Pacific oyster (*Crassostrea gigas*). In total, 16,458 nonredundant transcripts were classified into three major functional categories (biological process, molecular function, and cellular component) and 45 subcategories using the complete set of GO terms (Fig. 3). In the molecular function category, binding (8724, 53 %) was the most common, followed by catalytic activity (6128, 37.2 %). In the biological process category, cellular processes (8076, 44.1 %) comprised the largest proportion, followed by metabolic processes (6542, 35.7 %) and single-organism processes (5931, 32.4 %). Among the cellular component, the dominant clusters were cell (7857, 47.7 %) and organelle (5732, 34.9 %). Few genes were assigned to cell killing (12, 0.07 %), chemorepellent activity (1, 0.006 %), metallochaperone activity (5, 0.03 %), or virion (8, 0.05 %).

Table 3 De novo assembly statistics

Number of transcripts	53,121
Number of bases in transcript (Mbp)	31.79
Average length (bp)	599
N50	796
N80	342
Longest transcript (bp)	12,358

Table 4 Summary of *L. helicina* transcriptome annotation

	Number of transcripts
Sequences annotated with GO terms[a]	16,458
Significant BLASTx hits ($E < 1 \times 10^{-10}$) without GO terms	1177
Sequences with BLASTx hits ($1 \times 10^{-10} < E < 1 \times 10^{-3}$) without GO terms	689
No hits by BLASTx Search	34,797
Total	53,121

[a] These sequences contain 2898 transcripts with assigned EC numbers

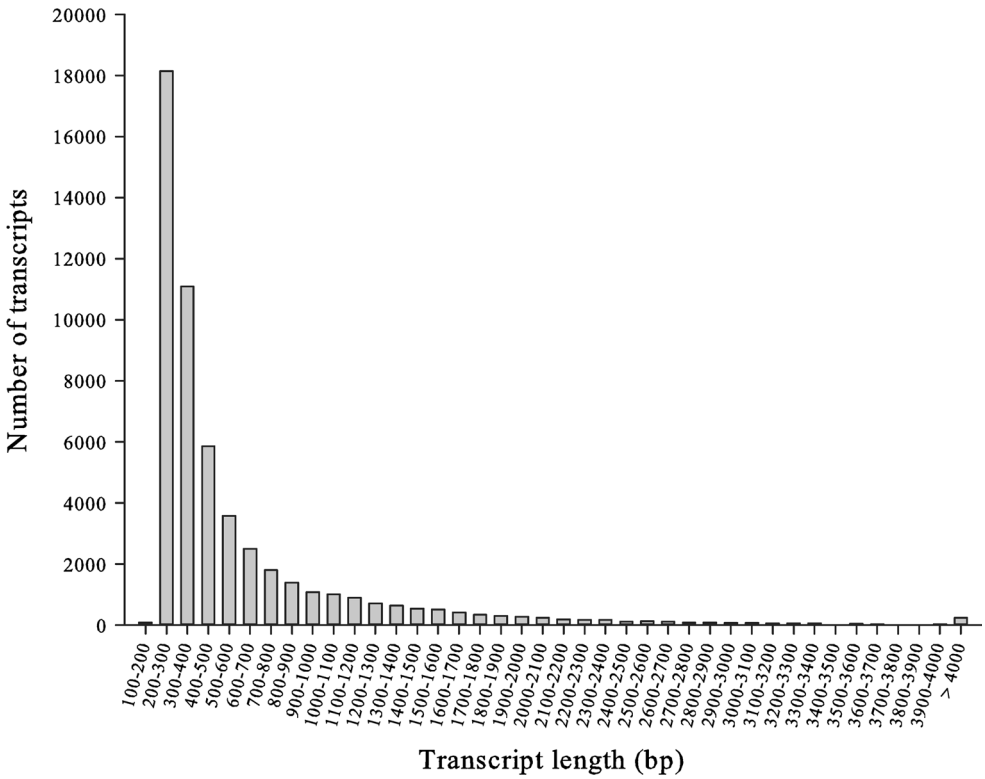

Fig. 1 Transcript length distribution of the Arctic pteropod *Limacina helicina* transcriptome

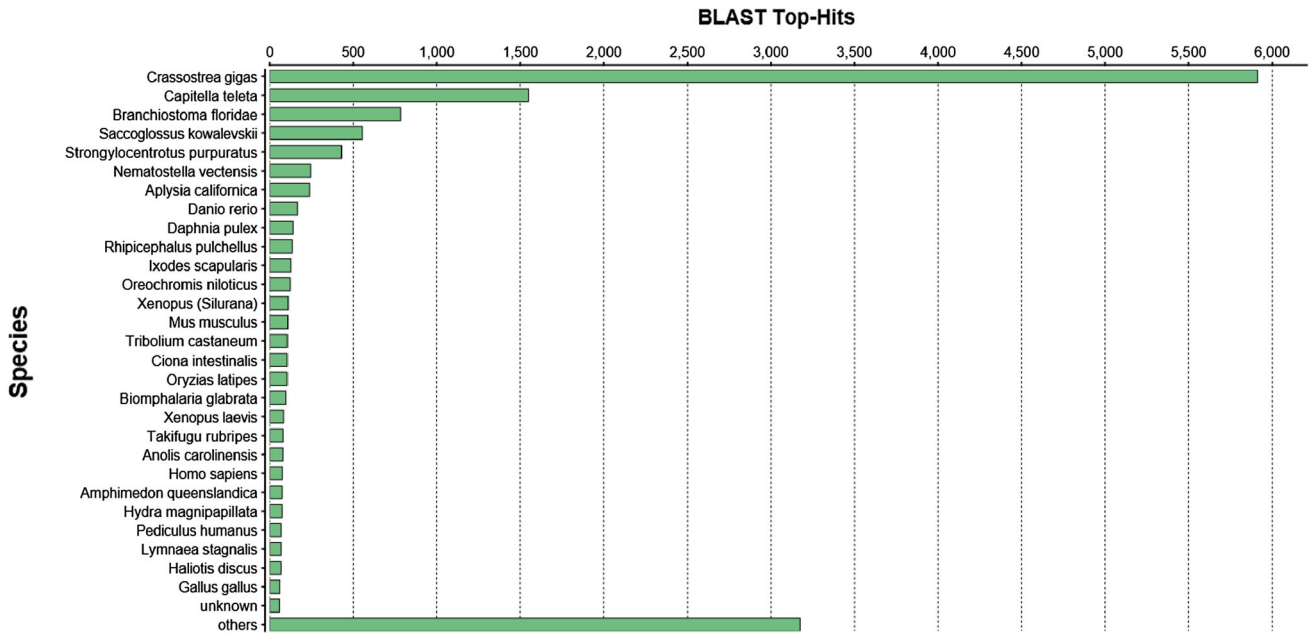

Fig. 2 Top BLASTx hit species distribution obtained against the NCBI nonredundant (nr) protein database. The number of top BLAST hits per species is presented

DEG analysis using expression profile

To identify DEGs induced by acidic stress in *L. helicina*, the overlap between the extreme CO_2- and high CO_2-driven acidic groups was investigated. A schematic transcriptome overlap is depicted in the form of a Venn diagram (Fig. 4). The data presented are the numbers of genes showing statistically significant more than twofold changes in abundance in the CO_2-driven acidic groups compared with the control group (Fig. 4). Among the upregulated genes, 346 (0.7 %) and 655 (1.2 %) genes responded to extreme-level CO_2 (pH 6.5) and high-level CO_2 (pH 7.5) conditions, respectively. Only 76 transcripts (0.1 %) were commonly upregulated in both conditions (Fig. 4a). Among the downregulated genes, 690 (1.3 %) and 739 (1.4 %) were so in response to extreme-level CO_2 and high-level CO_2, respectively (Fig. 4). Also, 270 genes (0.5 %) overlapped in both acidic stress conditions (Fig. 4b). The IDs of the transcript in each group are listed in ESM_1.

GO enrichment in DEGs

Subsets of DEGs were subjected to GO enrichment analysis (Table 5). The GO terms of regulation of respiratory burst (GO:0060263), negative regulation of endocytosis (GO:0045806), myoblast fusion (GO:0007520), and GTP-dependent protein binding (GO:0030742) were enriched in the upregulated transcript group. GO terms enriched in the downregulated group were fibrinolysis (GO:0042730), fibronectin binding (GO:0001968), beta-1,4-N-acetylgalactosaminyltransferase activity (GO: 0033842), extrinsic to external side of plasma membrane (GO:0031232), and extracellular region (GO:0005576). All enriched GO terms of the transcripts in each group are listed in ESM_2.

Contigs related to biomineralization in *L. helicina*

Biomineralization would be expected to be one of the major mechanisms used by *L. helicina* to cope with a shell-degrading acidic stress environment. As is common in shelled mollusks, possible biomineralization-related transcripts were found in *L. helicina*. Indeed, 14 representative transcripts showing differential expression are shown in Table 6. Fibrinogen, c-type lectin, cadherin domain protein, and cre-tyr-1 protein (tyrosinase) were downregulated under both high- and extreme-CO_2 conditions. Prism uncharacterized shell protein 1, chitinase 1, and nicotinic acetylcholine receptor were decreased only under extreme-CO_2 conditions. Transcript levels of collagen alpha-6 and sialic acid-binding lectin declined only in high-CO_2 conditions. Cysteine-rich protein, calmodulin family member-like, calmodulin 4, and dentin sialophosphoprotein precursor expression was increased in high-level CO_2 conditions. Chorion peroxidase was upregulated in extreme-CO_2 conditions. Several genes showed different expression in other isoforms, and all 504 biomineralization-related transcripts obtained from *L. helicina* in this study are listed in ESM_3.

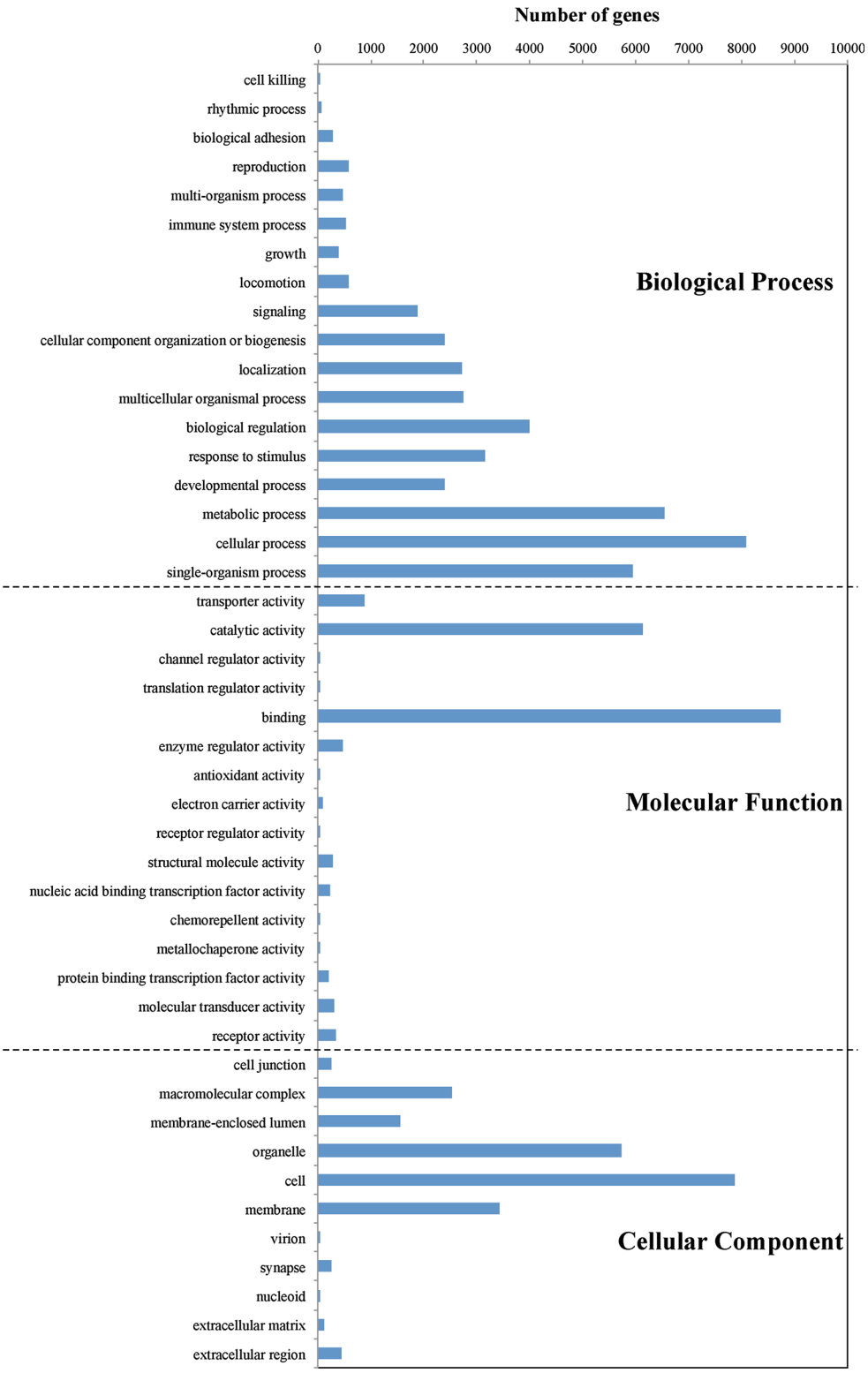

Fig. 3 Functional GO categorization of the *L. helicina* transcriptome. Sequences with BLASTx matches against the nr protein database were assigned GO terms and classified into the following three functional categories: biological process, molecular function, and cellular component

Analysis of acidic stress-induced gene expression by qRT-PCR

The transcript levels of six selected genes determined by DEG were validated by qRT-PCR, based on their high probability of differential expression under acidic stress (ESM_1). The six genes were amplified to the expected size (data not shown), suggesting that the assembly process was successful. β-Actin mRNA was expressed at similar levels in all samples obtained from normal and acidic

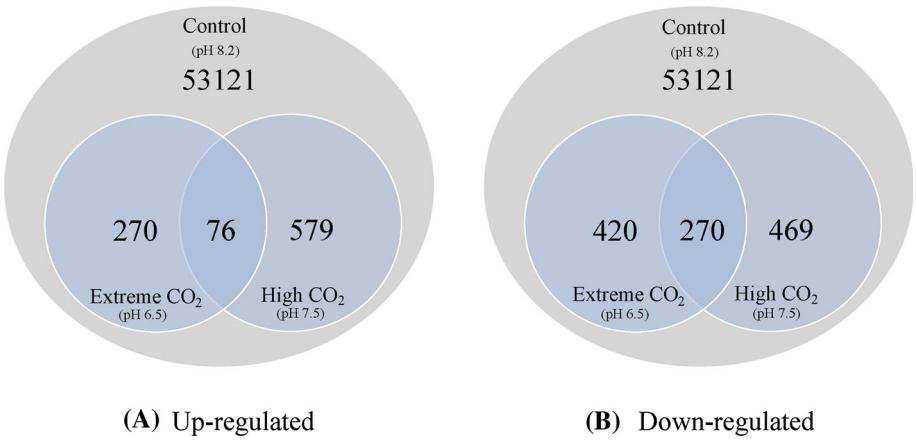

Fig. 4 DEG analysis of the *L. helicina* transcriptome exposed to high (pH 7.5) and extreme (pH 6.5) CO_2-driven acidification conditions. Venn diagram shows differentially expressed genes. Numbers of **a** upregulated genes and **b** downregulated genes

conditions (data not shown), making it an appropriate internal control gene for this study. Specifically, the PLG, alpha-amylase, Rac1, C-type lectin, cathepsin D, and collagen alpha-6 mRNA levels were measured by qRT-PCR (Fig. 5). Expression of a fibrinolysis-related plasma serine protease (PLG, plasminogen) and a small signaling G protein (Rac1), which are involved in cell proliferation and cytoskeletal reorganization, respectively, was upregulated significantly in both CO_2-driven acidic groups. The increase in PLG expression was identical under both high- and extreme-level CO_2 conditions. Moreover, the Rac1 mRNA level increased gradually in response to acidic conditions. The transcript of a polysaccharide-hydrolyzing enzyme (alpha-amylase) was upregulated under extreme-level CO_2 conditions. The expression of calcium-dependent carbohydrate-binding protein (C-type lectin) decreased significantly under both conditions. However, the transcript levels of an aspartic protease (cathepsin D) and the major structural protein of basement membrane (collagen alpha-6) declined only under high-CO_2 conditions. C-type lectin and collagen alpha-6 are involved in biomineralization (Livingston et al. 2006; Fang et al. 2011). These results were consistent with those from DEG profiling (ESM_1).

Discussion

Ocean acidification has affected biological systems in a broad range of marine habitats (Fabry et al. 2008). A recent study conducted a comprehensive meta-analysis on the effect of near-future ocean acidification among key taxonomic groups and showed that a broad range of marine organisms will be diminished in survival, calcification, growth, development, and abundance (Kroeker et al. 2013). Research has particularly shown that CO_2-driven ocean acidification may cause incomplete shell structures or even destroy shells (Feely et al. 2004; Orr et al. 2005b). Moreover, it could drive reduced growth or the death of marine calcifiers in harsh acidic environments (Miles et al. 2007; Van de Waal et al. 2013). In particular, shelled pteropods have been considered to be sensitive to acidified seawater because of their highly soluble, thin, fragile, aragonitic shells. The Arctic thecosomatous mollusk *L. helicina* is the only shelled pteropod in the Arctic Ocean. Reductions in their population may alter the Arctic marine ecosystem, and recent studies have focused on the impact of ocean acidification on this species (Comeau et al. 2010; Lischka et al. 2011; Comeau et al. 2012; Seibel et al. 2012; Busch et al. 2014). However, bioinformatics resources on the species, such as transcriptome or proteome information, have not been available before.

In the present study, we aimed to provide transcriptomic information on *L. helicina* in response to CO_2-driven acidification of arctic seawater using next-generation sequencing (NGS) technology. The Intergovernmental Panel on Climate Change for the year 2100 worst-case projection (A1FI) predicted the CO_2 emission scenarios representing anthropogenic CO_2 (Solomon et al. 2007); moreover, it was reported that natural CO_2 leaks out from geological sequestration sites, causing an extreme pH decrease to 5.6 (Porzio et al. 2011). The pH set ranges in this study were rather broad, but may reflect these both chances of CO_2-driven seawater acidification. It was shown that NGS technology makes reliable accordance with qRT-PCR and microarrays in DEG analysis of transcriptomes (Rothberg and Leamon 2008; Wang et al. 2009; Wilhelm and Landry 2009). The transcriptional expression of the selected genes from the differential expression profile of transcriptome was investigated by qRT-PCR (Fig. 5). About 65.5 % (34,797) of the transcripts showed no significant similarity to any sequence by BLAST searching against the currently available sequence pool (Table 4). This could be due in part to poorly conserved sequences from novel genes in this arctic pteropod. DEG analysis showed that numerous genes were significantly up- or

Table 5 Enrichment of GO terms of DEGs in *L. helicina* in response to CO_2-driven acidic conditions

GO term	Ontology[a]	Term	*p* value	False discovery rate (FDR)
I. Up-regulated				
GO:0010310	P	Regulation of hydrogen peroxide metabolic process	3.40E−15	2.10E−12
GO:0080010	P	Regulation of oxygen and reactive oxygen species metabolic process	3.40E−15	2.10E−12
GO:0035025	P	Positive regulation of Rho protein signal transduction	3.40E−15	2.10E−12
GO:0032627	P	Interleukin-23 production	7.10E−13	2.20E−10
GO:0032707	P	Negative regulation of interleukin-23 production	7.10E−13	2.20E−10
GO:0032667	P	Regulation of interleukin-23 production	7.10E−13	2.20E−10
GO:0060263	P	Regulation of respiratory burst	3.30E−11	8.60E−09
GO:0048261	P	Negative regulation of receptor-mediated endocytosis	5.80E−10	1.30E−07
GO:0045730	P	Respiratory burst	5.40E−09	1.10E−06
GO:0045806	P	Negative regulation of endocytosis	3.30E−08	6.10E−06
GO:0051668	P	Localization within membrane	1.40E−07	2.40E−05
GO:0006342	P	Chromatin silencing	4.90E−07	7.60E−05
GO:0000768	P	Syncytium formation by plasma membrane fusion	1.40E−06	0.00016
GO:0007520	P	Myoblast fusion	1.40E−06	0.00016
GO:0046579	P	Positive regulation of Ras protein signal transduction	1.40E−06	0.00016
GO:0045814	P	Negative regulation of gene expression, epigenetic	1.40E−06	0.00016
GO:0006949	P	Syncytium formation	3.50E−06	0.00038
GO:0042743	P	Hydrogen peroxide metabolic process	7.60E−06	0.0007
GO:0050690	P	Regulation of defense response to virus by virus	7.60E−06	0.0007
GO:0014902	P	Myotube differentiation	7.60E−06	0.0007
GO:0051057	P	Positive regulation of small GTPase-mediated signal transduction	1.50E−05	0.0013
GO:0050688	P	Regulation of defense response to virus	2.80E−05	0.0021
GO:0010592	P	Positive regulation of lamellipodium assembly	2.80E−05	0.0021
GO:0010591	P	Regulation of lamellipodium assembly	2.80E−05	0.0021
GO:0031529	P	Ruffle organization	7.70E−05	0.0057
GO:0051607	P	Defense response to virus	0.00026	0.018
GO:0002831	P	Regulation of response to biotic stimulus	0.00036	0.025
GO:0016574	P	Histone ubiquitination	0.00048	0.032
GO:0016160	F	Amylase activity	3.20E−70	6.90E−68
GO:0030742	F	GTP-dependent protein binding	3.30E−08	3.50E−06
GO:0031996	F	Thioesterase binding	7.70E−05	0.0055
GO:0016798	F	Hydrolase activity, acting on glycosyl bonds	0.00056	0.024
GO:0003727	F	Single-stranded RNA binding	0.00048	0.024
GO:0035064	F	Methylated histone residue binding	0.0011	0.038
GO:0051219	F	Phosphoprotein binding	0.0016	0.05
GO:0031519	C	PcG protein complex	7.60E−06	0.0011
II. Down-regulated				
GO:0043152	P	Induction of bacterial agglutination	4.30E−19	7.30E−16
GO:0042730	P	Fibrinolysis	1.20E−10	1.00E−07
GO:0030195	P	Negative regulation of blood coagulation	4.50E−10	2.50E−07
GO:0050819	P	Negative regulation of coagulation	1.10E−08	4.70E−06
GO:0030193	P	Regulation of blood coagulation	5.80E−08	2.00E−05
GO:0009247	P	Glycolipid biosynthetic process	3.60E−07	0.0001
GO:0050818	P	Regulation of coagulation	1.30E−06	0.00031
GO:0019731	P	Antibacterial humoral response	1.20E−05	0.0022

Table 5 continued

GO term	Ontology[a]	Term	*p* value	False discovery rate (FDR)
GO:0050829	P	Defense response to Gram-negative bacterium	1.20E−05	0.0022
GO:0006278	P	RNA-dependent DNA replication	2.60E−05	0.0045
GO:0044111	P	Development during symbiotic interaction	9.80E−05	0.011
GO:0044115	P	Development of symbiont during interaction with host	9.80E−05	0.011
GO:0009405	P	Pathogenesis	9.80E−05	0.011
GO:0051919	P	Positive regulation of fibrinolysis	9.80E−05	0.011
GO:0075015	P	Formation of infection structure on or near host	9.80E−05	0.011
GO:0006953	P	Acute-phase response	0.00041	0.044
GO:0001968	F	Fibronectin binding	6.30E−14	2.00E−11
GO:0034185	F	Apolipoprotein binding	4.10E−11	6.40E−09
GO:0034061	F	DNA polymerase activity	7.10E−08	7.50E−06
GO:0033842	F	N-acetyl-beta-glucosaminyl-glycoprotein 4-beta-N-acetylgalactosaminyltransferase activity	3.60E−07	2.80E−05
GO:0003964	F	RNA-directed DNA polymerase activity	4.20E−06	0.00026
GO:0016779	F	nucleotidyltransferase activity	0.00024	0.012
GO:0004252	F	Serine-type endopeptidase activity	0.00031	0.014
GO:0034358	C	Plasma lipoprotein particle	1.10E−08	1.30E−06
GO:0032994	C	Protein-lipid complex	1.10E−08	1.30E−06
GO:0031232	C	Extrinsic to external side of plasma membrane	9.80E−05	0.0058
GO:0005576	C	Extracellular region	7.90E−05	0.0058

[a] *P* biological process, *F* molecular function, *C* cellular component

downregulated under the elevated CO_2 conditions, reflecting putative molecular mechanisms of adaptation to acidic stress in *L. helicina*. Previous studies on corals revealed that increased CO_2 concentrations up- and downregulated the expression of the various Ras GTPase families (Kaniewska et al. 2012). Rac1 regulates cell motility and adhesion, cell cycle progression through G1, mitosis, and meiosis, and cell death and metastasis (Hall 2009). As shown in Fig. 5, upregulation of Rac1 suggests that cell membrane and cytoskeletal interactions are altered during acclimation to acidified seawater (Kaniewska et al. 2012). Alpha-amylases hydrolyze starch, but in some species, these enzymes digest alpha-D-(1,4)-linked polysaccharides, such as glycogen, in zooplankton (Mizutani et al. 2012). The differential expression of this transcript may explain energy metabolism in this pteropod, which could be changed in response to alterations in environmental conditions. Additionally, the cathepsin D transcript was downregulated in response to lowered pH. Cathepsin D is a lysosomal aspartic protease involved in cellular metabolism, degrading cellular and extracellular proteins, and activating proenzymes, prohormones, and growth factors (Bankowska et al. 1997), as well as melanization (Iwanaga and Lee 2005). In invertebrates, cathepsin D gene expression was upregulated in a calanoid copepod after nickel exposure to prevent cell death (Jiang et al. 2013). It is uncertain whether the differential expression of this gene in *L. helicina* is involved in cell fate. Plasminogen (PLG) is an inactive precursor of the trypsin-like serine protease plasmin. The plasminogen activator/plasmin system plays an important role in extracellular matrix (ECM) degradation (Liu 2008). In the purple sea urchin, plasminogen is likely involved in cellular clotting or coagulation of the coelomic fluid as an immune response (Hibino et al. 2006). Further functional studies should examine increased PLG gene expression in *L. helicina* at lower pH values.

The shell of most mollusks consists of an inner aragonitic nacreous layer and outer calcitic prismatic layer. These two layers are connected by the aragonitic line, where biomineralization is triggered. A recent study revealed that *L. helicina* has the thinnest shell among shelled gastropods, consisting of an outer prismatic layer, middle crossed-lamellar layer, and occasionally an inner prismatic layer (Sato-Okoshi et al. 2010). Although they possess very thin shells, the elastic and hard multiprismatic shell is resistant to chemical and mechanical effects. However, ocean acidification can lead to a reduced shell diameter in, and increased losses of, juvenile *L. helicina* (Lischka et al. 2011). Calcareous shells are critical for protection of thecosomatous pteropods against predators. The shells are essential in feeding, buoyancy control, pH regulation, and reproductive stage (Lalli and Gilmer 1989; Simkiss and

Table 6 Representative transcripts with homology to biomineralization-related genes in the *L. helicina*

Transcript ID	Description	cDNA length (bp)	Homologous genes No.	E-value	Homologous genes	Differential expression (fold)
Sample6-7_contig_27577	Fibrinogen	500	gil16303189	1.2217E−39	BgMFREP4 precursor (*Biomphalaria glabrata*)	High (−4.0) Extreme (−4.7)
Sample6-7_contig_2495	Cysteine-rich protein	3008	gil260785992	3.74898E−147	Hypothetical protein BRAFLDRAFT_123334 (*Branchiostoma floridae*)	High (4.2)
Sample6-7_contig_2915	Prism uncharacterized shell protein 1	1398	gil371782198	4.27378E−09	Prism uncharacterized shell protein 1 (*Pinctada margaritifera*)	Extreme (−3.9)
Sample6-7_contig_37523	CalModulin family member (cmd-1)-like, partial	740	gil291228246	4.05308E−13	CalModulin family member (cmd-1)-like, partial (*Saccoglossus kowalevskii*)	High (8.9)
Sample6-7_contig_21271[a]	Collagen alpha-6	1315	gil260797295	2.73707E−52	Hypothetical protein BRAFLDRAFT_235786 (*Branchiostoma floridae*)	High (−2.4)
Sample6-7_contig_26231[a]	c-type lectin domain family 11 member A-like	785	gil125845753	8.35297E−08	c-type lectin domain family 11 member A-like (*Danio rerio*)	High (−16.2) Extreme (−15.4)
Sample6-7_contig_2903	Cadherin domain protein	1043	gil260809731	1.03E−18	Hypothetical protein BRAFLDRAFT_205548 (*Branchiostoma floridae*)	High (−3.4) Extreme (−2.6)
Sample6-7_contig_9091	Calmodulin 4	988	gil306922665	1.36E−10	Calmodulin 4 (*Microtus ochrogaster*)	High (2.4)
Sample6-7_contig_7412	Chitinase 1	2962	gil198422580	8.65E−63	Similar to peritrophin 1 (*Ciona intestinalis*)	Extreme (−2.5)
Sample6-7_contig_48539	Nicotinic acetylcholine receptor partial	533	gil77020762	6.81E−95	Nicotinic acetylcholine receptor subunit type D (*Lymnaea stagnalis*)	Extreme (−9.1)
Sample6-7_contig_4721	Chorion peroxidase	2467	gil321470820	1.95E−101	Hypothetical protein DAPPUDRAFT_196036 (*Daphnia pulex*)	Extreme (3.5)
Sample6-7_contig_24813	Sialic acid-binding lectin	487	gil56606098	7.71E−13	Complement C1q subcomponent subunit C precursor (*Rattus norvegicus*)	High (−6.8)
Sample6-7_contig_10941	Dentin sialophosphoprotein precursor	1327	gil339635230	2.70E−09	Unnamed protein product (Weissella koreensis KACC 15510)	High (3.9)
Sample6-7_contig_4922	Cre-tyr-1 protein	1706	gil32452643	3.05E−52	Tyrosinase (*Sepia officinalis*)	High (−2.8) Extreme (−3.8)

[a] Transcripts used in qRT-PCR (Fig. 5)

Wilbur 1989). Considering the important function of shells, it is interesting that *L. helicina* synthesizes very thin shells. One possible reason is that lightweight shells are more acceptable for pelagic lifestyle of this pteropod (Sato-Okoshi et al. 2010). Although the shell of *L. helicina* is fragile in an acidified ocean environment, they maintain the shell formation mechanism by constructing rib structures (Sato-Okoshi et al. 2010), by biomineralization.

In this study, almost 1 % (504) of the transcripts showed sequence similarity to biomineralization-related genes (ESM_3). Among these transcripts, 16 genes showed differential expression in response to acidified seawater (Table 6). Differential expression of biomineralization-related genes can be inconsistent even in similar marine calcifiers. For example, increased expression of c-type lectin in cold-water coral (*Desmophyllum dianthus*) was reported when exposed to lower pH 7.7 for up to 8 months (Carreiro-Silva et al. 2014). However, decreased c-type lectin was recorded in another coral (*Acropora millepora*) in response to ocean acidification (Kaniewska et al. 2012).

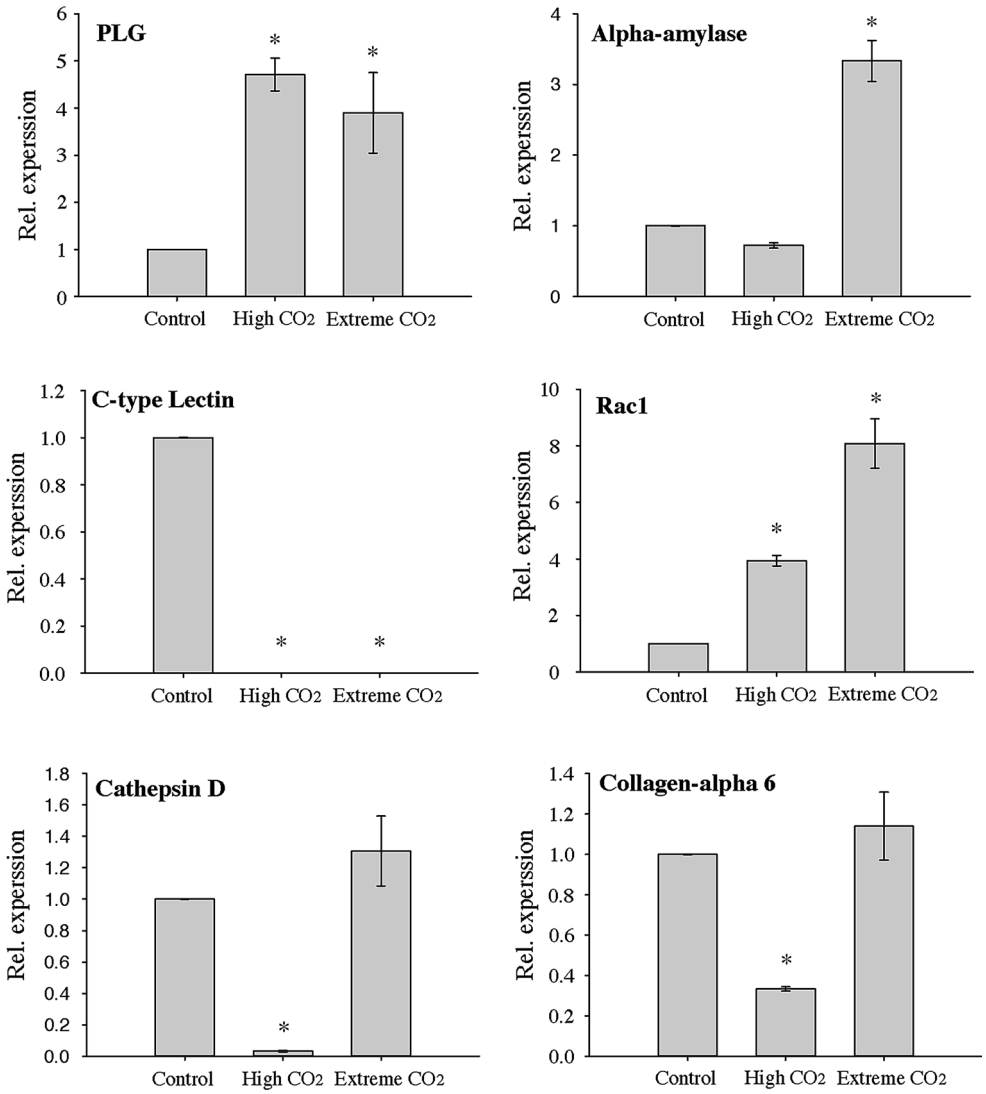

Fig. 5 qRT-PCR validation of selected genes affected by acidic stress. The *vertical axis* shows the relative expression levels of the indicated genes, compared with that of the reference gene (β-actin). *Error bars* indicate the SD of three independent replicates. *Asterisks* (*) indicate significant variation between the control and each acidified group ($p < 0.05$)

Similar decreases may occur in acid-stressed *L. helicina*, as found in the present study (Fig. 5). The up- and/or down-regulation of the expression of several genes differed according to the isoform (ESM_3). Moreover, most genes showed no significant difference under any condition tested. It is likely that constitutive expression of many biomineralization-related genes is necessary to maintain the basic shell structure, even in harsh environments. The isoforms of *L. helicina* transcripts that exhibited differential expression under acidic conditions could play important roles in mechanisms of adaptation to acidic stress. Furthermore, the different expression levels of gene isotypes may explain the seemingly inconsistent expression profiles reported elsewhere.

Future climate change driven by anthropogenic CO_2 could alter Arctic ecosystems, affecting Arctic food web networks. The polar oceans have been predicted to be the first to show undersaturation of $CaCO_3$—the Arctic Ocean within 10 years and the Antarctic Ocean in the next 20 years (Orr et al. 2005b; McNeil and Matear 2008; Steinacher et al. 2009). The transcriptome data sets for *L. helicina* subjected to acidic stress described herein contain information on genes whose expression was affected by increased CO_2, which is predicted in future environmental change. It is unsurprising that 504 transcripts (1 %) were identified as being biomineralization-related genes, because biomineralization is one of the key regulatory processes in most calcifiers. Nonetheless, the finding of biomineralization-related genes in the only Arctic shelled pteropod is described for the first time in this study. The impact on the only shelled pteropod in the Arctic Ocean—*L. helicina*—is particularly serious. Although most of the findings reported herein should be validated in functional studies, the data provide the first comprehensive overview of changes in transcript levels in the arctic pteropod *L. helicina* in response to CO_2-driven ocean acidification.

Acknowledgments We thank Young Deuk Han for field and laboratory assistance. This work was supported by the Grant from Korea Polar Research Institute (PE15070).

References

Bankowska A, Gacko M, Chyczewska E, Worowska A (1997) Biological and diagnostic role of cathepsin D. Rocz Akad Med Bialymst 42(Suppl 1):79–85

Bednarsek N, Feely RA, Reum JC, Peterson B, Menkel J, Alin SR, Hales B (2014) *Limacina helicina* shell dissolution as an indicator of declining habitat suitability owing to ocean acidification in the California Current Ecosystem. Proc Biol Sci 281:20140123

Berge JA, Bjerkeng B, Pettersen O, Schaanning MT, Øxnevad S (2006) Effects of increased sea water concentrations of CO_2 on growth of the bivalve *Mytilus edulis* L. Chemosphere 62:681–687

Berner RA, Honjo S (1981) Pelagic sedimentation of aragonite: its geochemical significance. Science 211:940–942

Busch DS, Maher M, Thibodeau P, McElhany P (2014) Shell condition and survival of puget sound pteropods are impaired by ocean acidification conditions. PLoS One 9:e105884

Carreiro-Silva M, Cerqueira T, Godinho A, Caetano M, Santos R, Bettencourt R (2014) Molecular mechanisms underlying the physiological responses of the cold-water coral *Desmophyllum dianthus* to ocean acidification. Coral Reefs 33:465–476

Collier R, Dymond J, Honjo S, Manganini S, Francois R, Dunbar R (2000) The vertical flux of biogenic and lithogenic material in the Ross Sea: moored sediment trap observations 1996–1998. Deep Sea Res Part 2 Top Stud Oceanogr 47:3491–3520

Comeau S, Gorsky G, Jeffree R, Teyssie JL, Gattuso J-P (2009) Impact of ocean acidification on a key Arctic pelagic mollusc (*Limacina helicina*). Biogeosciences 6:1877–1882

Comeau S, Jeffree R, Teyssie JL, Gattuso JP (2010) Response of the Arctic pteropod *Limacina helicina* to projected future environmental conditions. PLoS One 5:e11362

Comeau S, Gattuso JP, Nisumaa AM, Orr J (2012) Impact of aragonite saturation state changes on migratory pteropods. Proc Biol Sci 279:732–738

Conesa A, Götz S, García-Gómez JM, Terol J, Talón M, Robles M (2005) Blast2GO: a universal tool for annotation, visualization and analysis in functional genomics research. Bioinformatics 21:3674–3676

Conover RJ, Lalli CM (1972) Feeding and growth in *Clione limacina* (Phipps), a pteropod mollusc. J Exp Mar Biol Ecol 9:279–302

Doney SC, Fabry VJ, Feely RA, Kleypas JA (2009) Ocean acidification: the other CO_2 problem. Mar Sci 1:169–192

Du Z, Zhou X, Ling Y, Zhang Z, Su Z (2010) agriGO: a GO analysis toolkit for the agricultural community. Nucleic Acids Res 38:W64–W70

Dupont S, Havenhand J, Thorndyke W, Peck LS, Thorndyke M (2008) Near-future level of CO_2-driven ocean acidification radically affects larval survival and development in the brittlestar *Ophiothrix fragilis*. Mar Ecol Prog Ser 373:285–294

Evans TG, Chan F, Menge BA, Hofmann GE (2013) Transcriptomic responses to ocean acidification in larval sea urchins from a naturally variable pH environment. Mol Ecol 22:1609–1625

Fabry VJ, Seibel BA, Freely RA, Orr JC (2008) Impacts of ocean acidification on marine fauna and ecosystem processes. ICES J Mar Sci 65:414–432

Fang D, Xu G, Hu Y, Pan C, Xie L, Zhang R (2011) Identification of genes directly involved in shell formation and their functions in pearl oyster, *Pinctada fucata*. PLoS One 6:e21860

Feely RA, Sabine CL, Lee K, Berelson W, Kleypas J, Fabry VJ, Millero FJ (2004) Impact of anthropogenic CO_2 on the $CaCO_3$ system in the oceans. Science 305:362–366

Fu FX, Warner ME, Zhang Y, Feng Y, Hutchins DA (2007) Effects of increased temperature and CO_2 on photosynthesis, growth, and elemental ratios in marine *Synechococcus* and *Prochlorococcus* (Cyanobacteria). J Phycol 43:485–496

Gannefors C, Böer M, Kattner G, Graeve M, Eiane K, Gulliksen B, Hop H, Falk-Petersen S (2005) The Arctic sea butterfly *Limacina helicina*: lipids and life strategy. Mar Biol 147:169–177

Gattuso J-P, Frankignoulle M, Bourge I, Romaine S, Buddemeier R (1998) Effect of calcium carbonate saturation of seawater on coral calcification. Global Planet Change 18:37–46

Gazeau F, Quiblier C, Jansen JM, Gattuso JP, Middelburg JJ, Heip CH (2007) Impact of elevated CO_2 on shellfish calcification. Geophys Res Lett 34:L07603

Gilmer RW (1990) In situ observations of feeding behavior of thecosome pteropod molluscs. Am Malacol Bull 8:53–59

Gilmer R, Harbison G (1986) Morphology and field behavior of pteropod molluscs: feeding methods in the families Cavoliniidae, Limacinidae and Peraclididae (Gastropoda: Thecosomata). Mar Biol 91:47–57

Gilmer R, Harbison G (1991) Diet of *Limacina helicina*(Gastropoda: Thecosomata) in Arctic waters in midsummer. Mar Ecol Prog Ser 77:125–134

Grabherr MG, Haas BJ, Yassour M, Levin JZ, Thompson DA, Amit I, Adiconis X, Fan L, Raychowdhury R, Zeng Q (2011) Full-length transcriptome assembly from RNA-Seq data without a reference genome. Nat Biotechnol 29:644–652

Hall A (2009) The cytoskeleton and cancer. Cancer Metastasis Rev 28:5–14

Hamner WM, Madin LP, Alldredge AL, Gilmer RW, Hamner PP (1975) Underwater observations of gelatinous zooplankton: sampling problems, feeding biology, and behavior. Limnol Oceanogr 20:907–917

Harris JO, Maguire GB, Edwards SJ, Hindrum SM (1999) Effect of pH on growth rate, oxygen consumption rate, and histopathology of gill and kidney tissue for juvenile greenlip abalone, *Haliotis laevigata* Donovan and blacklip abalone, *Haliotis rubra* Leach. J Shellfish Res 18:611–619

Hauton C, Tyrrell T, Williams J (2009) The subtle effects of sea water acidification on the amphipod *Gammarus locusta*. Biogeosciences 6:1479–1489

Hibino T, Loza-Coll M, Messier C, Majeske AJ, Cohen AH, Terwilliger DP, Buckley KM, Brockton V, Nair SV, Berney K, Fugmann SD, Anderson MK, Pancer Z, Cameron RA, Smith LC, Rast JP (2006) The immune gene repertoire encoded in the purple sea urchin genome. Dev Biol 300:349–365

Hunt B, Pakhomov E, Hosie G, Siegel V, Ward P, Bernard K (2008) Pteropods in southern ocean ecosystems. Prog Oceanogr 78:193–221

Iwanaga S, Lee B-L (2005) Recent advances in the innate immunity of invertebrate animals. BMB Rep 38:128–150

Jiang JL, Wang GZ, Mao MG, Wang KJ, Li SJ, Zeng CS (2013) Differential gene expression profile of the calanoid copepod, *Pseudodiaptomus annandalei*, in response to nickel exposure. Comp Biochem Physiol C Toxicol Pharmacol 157:203–211

Kaniewska P, Campbell PR, Kline DI, Rodriguez-Lanetty M, Miller DJ, Dove S, Hoegh-Guldberg O (2012) Major cellular and physiological impacts of ocean acidification on a reef building coral. PLoS One 7:e34659

Karnovsky NJ, Hobson KA, Iverson S, Hunt G (2008) Seasonal changes in diets of seabirds in the North Water Polynya: a multiple-indicator approach. Mar Ecol Prog Ser 357:291

Kroeker KJ, Kordas RL, Crim R, Hendriks IE, Ramajo L, Singh GS, Duarte CM, Gattuso JP (2013) Impacts of ocean acidification on marine organisms: quantifying sensitivities and interaction with warming. Glob Chang Biol 19:1884–1896

Kurihara H, Shirayama Y (2004) Effects of increased atmospheric CO_2 on sea urchin early development. Mar Ecol Prog Ser 274:161–169

Kurihara H, Kato S, Ishimatsu A (2007) Effects of increased seawater pCO_2 on early development of the oyster *Crassostrea gigas*. Aquat Biol 1:91–98

Lalli CM, Gilmer RW (1989) Pelagic snails: the biology of holoplanktonic gastropod mollusks. Stanford University Press, Stanford

Langdon C, Atkinson M (2005) Effect of elevated pCO_2 on photosynthesis and calcification of corals and interactions with seasonal change in temperature/irradiance and nutrient enrichment. J Geophys Res 110:C09S07

Langmead B, Trapnell C, Pop M, Salzberg SL (2009) Ultrafast and memory-efficient alignment of short DNA sequences to the human genome. Genome Biol 10:R25

Larson RJ, Harbison GR (1989) Source and fate of lipids in polar gelatinous zooplankton. Arctic 42:339–346

Leng N, Dawson JA, Thomson JA, Ruotti V, Rissman AI, Smits BM, Haag JD, Gould MN, Stewart RM, Kendziorski C (2013) EBSeq: an empirical Bayes hierarchical model for inference in RNA-seq experiments. Bioinformatics 29:1035–1043

Li B, Dewey CN (2011) RSEM: accurate transcript quantification from RNA-Seq data with or without a reference genome. BMC Bioinformatics 12:323

Lischka S, Büdenbender J, Boxhammer T, Riebesell U (2011) Impact of ocean acidification and elevated temperatures on early juveniles of the polar shelled pteropod *Limacina helicina*: mortality, shell degradation, and shell growth. Biogeosciences 8:919–932

Liu R-M (2008) Oxidative stress, plasminogen activator inhibitor 1, and lung fibrosis. Antioxid Redox Signal 10:303–320

Livingston BT, Killian CE, Wilt F, Cameron A, Landrum MJ, Ermolaeva O, Sapojnikov V, Maglott DR, Buchanan AM, Ettensohn CA (2006) A genome-wide analysis of biomineralization-related proteins in the sea urchin *Strongylocentrotus purpuratus*. Dev Biol 300:335–348

McNeil BI, Matear RJ (2008) Southern Ocean acidification: a tipping point at 450-ppm atmospheric CO_2. Proc Natl Acad Sci USA 105:18860–18864

Michaelidis B, Ouzounis C, Paleras A, Pörtner HO (2005) Effects of long-term moderate hypercapnia on acid-base balance and growth rate in marine mussels *Mytilus galloprovincialis*. Mar Ecol Prog Ser 293:109–118

Miles H, Widdicombe S, Spicer JI, Hall-Spencer J (2007) Effects of anthropogenic seawater acidification on acid-base balance in the sea urchin *Psammechinus miliaris*. Mar Pollut Bull 54:89–96

Mizutani K, Toyoda M, Otake Y, Yoshioka S, Takahashi N, Mikami B (2012) Structural and functional characterization of recombinant medaka fish alpha-amylase expressed in yeast *Pichia pastoris*. Biochim Biophys Acta 1824:954–962

Moy AD, Howard WR, Bray SG, Trull TW (2009) Reduced calcification in modern Southern Ocean planktonic foraminifera. Nat Geosci 2:276–280

Orr JC, Fabry VJ, Aumont O, Bopp L, Doney SC, Feely RA, Gnanadesikan A, Gruber N, Ishida A, Joos F (2005a) Anthropogenic ocean acidification over the twenty-first century and its impact on calcifying organisms. Nature 437:681–686

Orr JC, Fabry VJ, Aumont O, Bopp L, Doney SC, Feely RA, Gnanadesikan A, Gruber N, Ishida A, Joos F, Key RM, Lindsay K, Maier-Reimer E, Matear R, Monfray P, Mouchet A, Najjar RG, Plattner GK, Rodgers KB, Sabine CL, Sarmiento JL, Schlitzer R, Slater RD, Totterdell IJ, Weirig MF, Yamanaka Y, Yool A (2005b) Anthropogenic ocean acidification over the twenty-first century and its impact on calcifying organisms. Nature 437:681–686

Pörtner H-O, Reipschläger A, Heisler N (1998) Acid-base regulation, metabolism and energetics in *Sipunculus nudus* as a function of ambient carbon dioxide level. J Exp Biol 201:43–55

Porzio L, Buia MC, Hall-Spencer JM (2011) Effects of ocean acidification on macroalgal communities. J Exp Mar Biol Ecol 400:278–287

Quevillon E, Silventoinen V, Pillai S, Harte N, Mulder N, Apweiler R, Lopez R (2005) InterProScan: protein domains identifier. Nucleic Acids Res 33:W116–W120

Reipschläger A, Pörtner H (1996) Metabolic depression during environmental stress: the role of extracellular versus intracellular pH in *Sipunculus nudus*. J Exp Biol 199:1801–1807

Riebesell U, Zondervan I, Rost B, Tortell PD, Zeebe RE, Morel FM (2000) Reduced calcification of marine plankton in response to increased atmospheric CO2. Nature 407:364–367

Roberts D, Howard WR, Roberts JL, Bray SG, Moy AD, Trull TW, Hopcroft RR (2014) Diverse trends in shell weight of three Southern Ocean pteropod taxa collected with Polar Frontal Zone sediment traps from 1997 to 2007. Polar Biol 37:1445–1458

Robinson MD, Oshlack A (2010) A scaling normalization method for differential expression analysis of RNA-seq data. Genome Biol 11:R25

Rokitta SD, John U, Rost B (2012) Ocean acidification affects redox-balance and ion-homeostasis in the life-cycle stages of *Emiliania huxleyi*. PLoS One 7:e52212

Rosa R, Seibel BA (2008) Synergistic effects of climate-related variables suggest future physiological impairment in a top oceanic predator. Proc Natl Acad Sci USA 105:20776–20780

Rothberg JM, Leamon JH (2008) The development and impact of 454 sequencing. Nat Biotechnol 26:1117–1124

Sabine CL, Feely RA, Gruber N, Key RM, Lee K, Bullister JL, Wanninkhof R, Wong CS, Wallace DW, Tilbrook B, Millero FJ, Peng TH, Kozyr A, Ono T, Rios AF (2004) The oceanic sink for anthropogenic CO_2. Science 305:367–371

Sato-Okoshi W, Okoshi K, Sasaki H, Akiha F (2010) Shell structure of two polar pelagic molluscs, Arctic *Limacina helicina* and Antarctic *Limacina helicina antarctica* forma *antarctica*. Polar Biol 33:1577–1583

Seibel BA, Maas AE, Dierssen HM (2012) Energetic plasticity underlies a variable response to ocean acidification in the pteropod, *Limacina helicina antarctica*. PLoS One 7:e30464

Shirayama Y, Thornton H (2005) Effect of increased atmospheric CO_2 on shallow water marine benthos. J Geophys Res 110:C09S08

Simkiss K, Wilbur K (1989) Biomineralization: cell biology and mineral deposition. Academic Press, San Diego

Solomon S, Qin D, Manning M, Marquis M, Averyt K, Tignor MMB, Miller HL, Chen Z (eds) (2007) Climate change 2007 - The physical science basis: contribution of working group I to the fourth assessment report of the intergovernmental panel on climate change. Cambridge University Press, Cambridge, 996 pp

Steinacher M, Joos F, Frolicher T, Plattner G, Doney S (2009) Imminent ocean acidification in the Arctic projected with the NCAR global coupled carbon cycle-climate model. Biogeosciences 6:515–533

Todgham AE, Hofmann GE (2009) Transcriptomic response of sea urchin larvae *Strongylocentrotus purpuratus* to CO_2-driven seawater acidification. J Exp Biol 212:2579–2594

Van de Waal DB, John U, Ziveri P, Reichart GJ, Hoins M, Sluijs A, Rost B (2013) Ocean acidification reduces growth and calcification in a marine dinoflagellate. PLoS One 8:e65987

Wang Z, Gerstein M, Snyder M (2009) RNA-Seq: a revolutionary tool for transcriptomics. Nat Rev Genet 10:57–63

Watanabe Y, Yamaguchi A, Ishida H, Harimoto T, Suzuki S, Sekido Y, Ikeda T, Shirayama Y, Mac Takahashi M, Ohsumi T (2006) Lethality of increasing CO_2 levels on deep-sea copepods in the western North Pacific. J Oceanogr 62:185–196

Wilhelm BT, Landry JR (2009) RNA-Seq-quantitative measurement of expression through massively parallel RNA-sequencing. Methods 48:249–257